A Statistical Description of Small-Scale Turbulence in the Low-Level Nocturnal Jet

ROD FREHLICH, YANNICK MEILLIER, MICHAEL L. JENSEN, AND BEN BALSLEY

Cooperative Institute for Research in the Environmental Sciences, University of Colorado, Boulder, Colorado

(Manuscript received 3 April 2003, in final form 1 December 2003)

ABSTRACT

The probability density function (PDF) and spatial statistics of both the energy dissipation rate ϵ and the temperature structure constant C_T^2 are determined for the shear region of a nocturnal jet. The PDF of ϵ and C_T^2 are approximately lognormal. In addition, the joint probability density function of ϵ and C_T^2 is approximately a joint lognormal distribution. The one-dimensional spatial spectra of ϵ and C_T^2 in the inertial region have a $k^{-0.5}$ and $k^{-0.6}$ dependence, respectively, where k is the horizontal spatial wavenumber.

1. Introduction

The Cooperative Atmosphere–Surface Exchange Study 1999 (CASES-99) was conducted to investigate the atmospheric processes of the nocturnal boundary layer near Leon, Kansas, east (50 km) of Wichita, Kansas, during the month of October 1999 (Poulos et al. 2002). An important aspect of stable nighttime turbulence is the ''global intermittency'' (Mahrt 1989), that is, variations in space and time of the finescale turbulence quantities such as the energy dissipation rate ϵ and the temperature structure constant C_T^2. Muschinski and Lenschow (2001) have produced an overview of the various research needs in the area of finescale turbulence and some of these needs were addressed by the CASES-99 campaign (Poulos et al. 2002).

The small-scale velocity statistics of turbulence were predicted for locally stationary and isotropic conditions by Kolmogorov (1941) over 60 years ago assuming that the average energy dissipation rate ϵ was constant over a spatial domain less than the external length scale L. Kolmogorov (1962) proposed a refined similarity theory to include the random variations of ϵ. The key predictions of this theory are based on the probability density function (PDF) of ϵ as well as the spatial statistics of ϵ such as the spatial correlation B_ϵ and the spatial spectrum S_ϵ. Various models for the PDF of ϵ have been proposed including the lognormal distribution and fractal distributions (Kolmogorov 1962; Van Atta 1971; Mandelbrot 1991; Frisch 1995). Numerous predictions of turbulence statistics have been produced based on the refined similarity theory and the fundamental quantity is the intermittency exponent μ, which can be defined in terms of the spatial covariance of ϵ, the spatial spectrum of ϵ, the variance of log ϵ, the second moment of ϵ, and other statistics (Kolmogorov 1962; Yaglom 1966; Novikov and Stewart 1964; Nelkin 1981; Sreenivasan and Kailasnath 1993). Variations of ϵ and C_T^2 affect the interpretation of the small-scale statistics of turbulence (Yaglom 1966; Van Atta 1971; Sreenivasan and Stolovitzky 1996; Alisse and Sidi 2000).

The statistical description of the variations in ϵ and C_T^2 are essential for valid comparison with other remote sensing techniques for estimating ϵ or C_T^2 because remote sensing estimates are produced as a spatial average of the turbulent field. The most common remote sensing measurements of ϵ include Doppler radar (Cohn 1995; Jacoby-Koaly et al. 2002) and Doppler lidar (Frehlich et al. 1998). Estimates of C_n^2, which is proportional to C_T^2, are produced by sodar (Gossard et al. 1984; Smedman 1988) and frequency-modulated continuous wave (FMCW) radar (Richter 1969; Gossard et al. 1984; Eaton et al. 1995). Variations in small-scale turbulence are also important for many problems of wave propagation in random media (Tatarskii 1971), such as imaging (Roddier 1981) and adaptive optics (Tyson 1991).

In situ measurements of the small-scale turbulence are typically performed with fixed sensors on towers or on moving platforms such as aircraft. Both measurements are limited in their altitude coverage and aircraft provide measurements at a single altitude. In addition, to sample a given regime of spatial scale, measurements from a fast moving aircraft platform require wider bandwidth and lower noise than the same measurements from a slow moving platform (Muschinski et al. 2001). The tethered lifting system (TLS) was developed by the Cooperative Institute for Research in the Environmental Sciences (CIRES) at the University of Colorado for a variety of atmospheric measurements (Balsley et al.

Corresponding author address: Dr. Rod Frehlich, CIRES, Campus Box 216, University of Colorado, Boulder, CO 80309.
E-mail: rgf@cires.colorado.edu

1998, 2003; Muschinski et al. 2001). A vertical array of sensors was specifically designed for the CASES-99 campaign to produce finescale temperature and velocity measurements. These measurements could be made at fixed altitudes by keeping the platform stationary or by slowly moving the platform to produce profiles of atmospheric quantities from the surface up to an altitude of 2 km (see Fig. 1 of Balsley et al. 2003). Temperature measurements were produced with a low-frequency response solid-state temperature sensor and a high-frequency response fine cold-wire sensor. Velocity measurements were made using a sensitive Pitot-tube velocity sensor vaned into the wind and a high-frequency response fine hot-wire sensor. Both cold-wire and hot-wire signals were sampled at 200 Hz. The temperature was calibrated to an absolute accuracy better than 0.5 K and the accuracy of the linear calibration constant was better than 2%. The velocity was calibrated to an absolute accuracy of better than 1 m s^{-1} and the accuracy of the slope of the calibration curve is better than 5% (Frehlich et al. 2003). This resulting dataset permits accurate spectral-based estimates of the temperature and velocity structure constants (C_T^2 and $\epsilon^{2/3}$) that describe the small-scale turbulence (Frehlich et al. 2003). The sampling error of the estimates for the spectral level in the inertial range ($\epsilon^{2/3}$ and C_T^2) is typically 15% using 1 s of data. In this study, the statistics of both ϵ and C_T^2 will be calculated for the shear region of a nocturnal jet using high-resolution in situ estimates.

2. Turbulence conditions in the nocturnal jet

Accurate measurements of turbulence statistics require a sufficiently long stationary time series. An ideal dataset using the TLS during CASES-99 was collected from 10–12 UTC on 21 October 1999. During this period, four turbulence sensor packages with a separation of 6 m and numbered 1, 2, 3, and 5 were suspended at altitudes between 50–70 m. A stable nocturnal jet was present with a mean velocity of 6 m s^{-1} and a vertical shear of approximately 0.045 s^{-1} with the nose of the jet located the at an altitude of 90 m. The gradient Richardson number is between 0.4 and 1 for the altitude range of the data, indicating moderately stable conditions (Balsley et al. 2003).

In general, the small-scale statistics of the velocity field are well described by the structure function

$$D_u(s) = \langle [u(x) - u(x + s)]^2 \rangle, \tag{1}$$

where $u(x)$ is the longitudinal or streamwise velocity fluctuations; that is, the velocity component in the direction of the mean velocity vector **U** and s denotes the separation distance along the flow. Similarly, the temperature structure function is given by

$$D_T(s) = \langle [T(x) - T(x + s)]^2 \rangle, \tag{2}$$

where $T(x)$ is the temperature. For large Reynolds number flows and for separations s in the inertial range of the velocity field defined by $\eta < s < L_u$,

$$D_u(s) = C_K \epsilon^{2/3} s^{2/3}, \tag{3}$$

where ϵ is the energy dissipation rate, $\eta = \nu^{3/4}/\epsilon^{1/4}$ is the dissipation scale, ν is the kinematic viscosity, $C_K \approx 2.0$ is the Kolmogorov constant, and L_u is the outer scale that defines the dimensions of the largest energy-containing eddies. Similarly, for separations in the inertial range of the temperature field defined by $\eta_T < s < L_T$,

$$D_T(s) = C_T^2 s^{2/3}, \tag{4}$$

where C_T^2 is the temperature structure constant, $\eta_T = \chi^{3/4}/\epsilon^{1/4}$ is the dissipation scale for temperature, χ is the thermal diffusivity of air, and L_T is the outer scale for temperature fluctuations.

Since the velocity and temperature fields are continuous, for small separation (Monin and Yaglom 1975; 353, 385),

$$D_u(s) = \frac{\epsilon}{15\nu} s^2 \qquad s \ll \eta, \quad \text{and} \tag{5}$$

$$D_T(s) = \frac{N}{3\chi} s^2 \qquad s \ll \eta_T, \tag{6}$$

where N is the rate of dissipation of temperature variance. Equation (5) can be used to estimate ϵ.

For separations much larger than L_u, $D_u(s) = 2\sigma_u^2$ where σ_u^2 is the variance of the longitudinal velocity. Similarly, for separations much larger than L_T, $D_T(s) = 2\sigma_T^2$, where σ_T^2 is the variance of the temperature fluctuations. The length scales L_u and L_T are defined as the separation where the inertial range scaling Eqs. (7) and (8) intersect the constant level of the structure functions at large separation. The velocity length scale L_u is given by

$$L_u = \sigma_u^3/\epsilon, \tag{7}$$

and the temperature length scale L_T is

$$L_T = 2^{3/2}\sigma_T^3/C_T^{3/2}. \tag{8}$$

The structure functions of the longitudinal velocity and temperature are shown in Fig. 1 for sensor package 5 located at an altitude of 58 m. The spatial statistics are determined from the temporal statistics assuming Taylor's frozen flow hypothesis is valid (Taylor 1938; Monin and Yaglom 1975, p. 365; Wyngaard and Clifford 1977; Hill 1996). This is a good approximation since $\sigma_u \approx 0.14$ m s^{-1}, $U \approx 6.0$ m s^{-1}, and $\sigma_u/U \approx 0.0235 \ll 1$. The velocity and temperature length scales can be estimated from the structure functions. For velocity L_u is approximately 10 m [see Eq. (7) with $\sigma_u \approx 0.02$ and $\epsilon = 0.000\ 344$ m^2 s^{-3}] and for temperature the length scale L_T is approximately 20 m [see Eq. (8) with $\sigma_T \approx 0.1$ K and $C_T^2 = 0.002\ 365$ K^2 $m^{-2/3}$]. As indicated by the departure of the linear slope of the log–log plots at small spacing, both structure functions display the be-

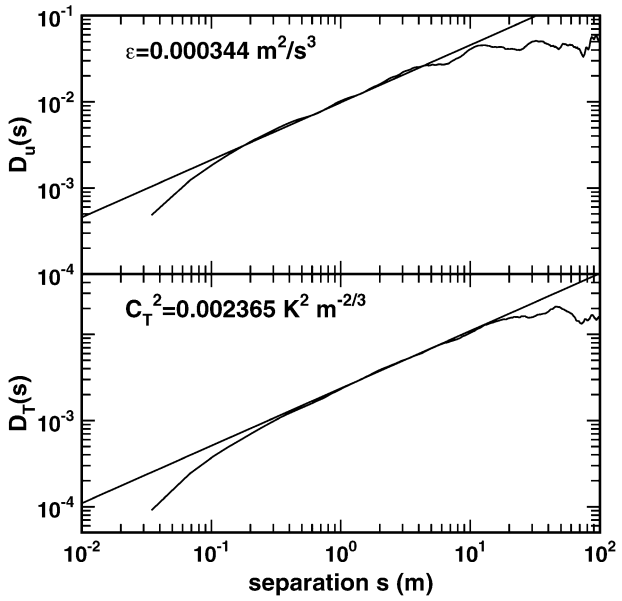

FIG. 1. Structure functions of longitudinal velocity $D_u(s)$ and temperature $D_T(s)$ vs separation distance s for a turbulent field in a nocturnal jet. Estimates of the energy dissipation rate ϵ and temperature structure constant C_T^2 are indicated, as well as the inertial range scaling.

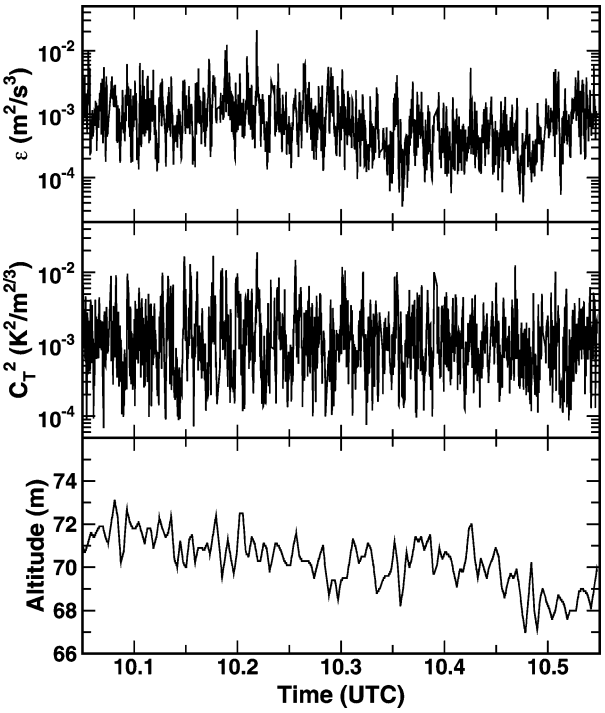

FIG. 2. Examples of a time series of 1-s estimates of (top) energy dissipation rate ϵ, (middle) temperature structure constant C_T^2, and (bottom) the altitude of sensor package 3.

ginning of the dissipation range scaling Eqs. (5) and (6). Unfortunately, the required square-law scaling for small spacing is not resolved and the dissipation scales cannot be directly measured. Both structure functions display the classic inertial range of Eqs. (3) and (4). Note that in the inertial range there is no statistically significant deviation from the classic inertial range slope of 2/3. The refined similarity theory predicts a slope of $2/3 + \mu/9$ where μ is the intermittency exponent (Yaglom 1966). Praskovsky and Oncley (1994) also produced $\mu \approx 0$ based on measurements of the spatial spectrum of velocity in high Reynolds number flows. Therefore, we define the small-scale turbulence by the level of the inertial range assuming the slope of 2/3 for the structure function and $-5/3$ for the spectrum. The estimates of ϵ and C_T^2 are produced with the maximum likelihood estimator in the spectral domain for optimal statistical accuracy, which is critical for short time intervals (Smalikho 1997; Ruddick et al. 2000; Frehlich et al. 2003). The statistical description of these estimates of small-scale turbulence is the focus of this work.

To determine the turbulent conditions of the measurements, we assume isotropic turbulence and estimate Taylor's Reynolds number, which is then given by

$$R_\lambda = \sigma_u \lambda/\nu = \sigma_u^2 \sqrt{15/(\nu\epsilon)}, \tag{9}$$

where the Taylor microscale

$$\lambda = \sigma_u / \langle (\partial u/\partial x)^2 \rangle^{1/2} = \sigma_u \sqrt{15\nu/\epsilon}, \tag{10}$$

and $\nu \approx 1.50 \times 10^{-5}$ m^2 s^{-1} is the kinematic viscosity calculated from the atmospheric conditions (Frehlich et al. 2003). For the velocity structure function of Fig. 1, $\sigma_u^2 \approx 0.02$ m^2 s^{-2}, $\epsilon = 3.44 \times 10^{-4}$ m^2 s^{-3}, so that $R_\lambda \approx 1078$ and the dissipation scale $\eta \approx 1.77$ mm. Although conditions vary with time, for most of the data the Reynolds number is larger than 500, that is, high Reynolds number flow. The dissipation scale for temperature $\eta_T \approx 2.28$ mm using the calculated value of $\chi = 2.10 \times 10^{-5}$ m^2 s^{-1}.

3. PDF of small-scale turbulence

A long period of stationary data is required for investigating the statistical variability of small-scale turbulence. Time series of 1-s estimates of ϵ and C_T^2 from sensor package 3 are shown in Fig. 2 for 30 min of data (Frehlich et al. 2003). The altitude of the measurements is approximately 70 m with low-frequency variations on the order of a few meters. Since the wind speed is measured with respect to the sensor package and Taylor's frozen hypothesis (Taylor 1938; Wyngaard and Clifford 1977; Hill 1996) is valid ($\sigma_u/U \approx 0.0235 \ll 1$), these low-frequency variations of the package motion are negligible. The variability in ϵ and C_T^2 is dominated by the intrinsic turbulent variability because the estimation error of each measurement is typically less than 15% (Frehlich et al. 2003). The fluctuations in $\ln(C_T^2)$ are very stationary, while there is some low-frequency variations observable in $\ln(\epsilon)$. To remove the small effects of these low-frequency variations and to

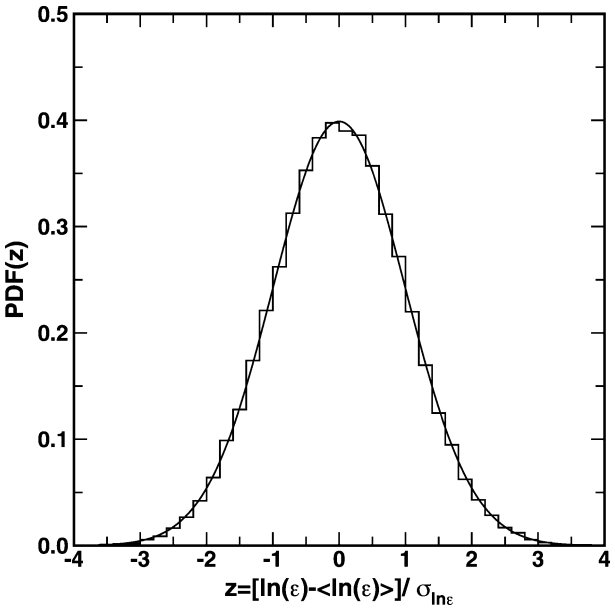

FIG. 3. PDF of $\ln\epsilon$ and the prediction of the lognormal distribution.

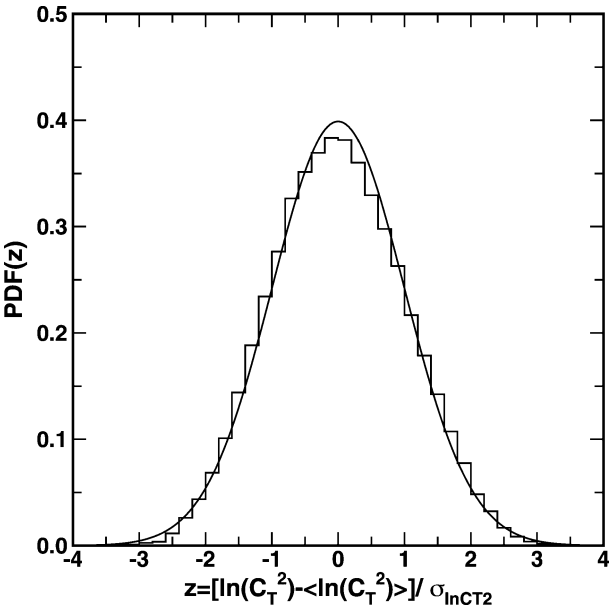

FIG. 4. PDF of $\ln C_T^2$ and the prediction of the lognormal distribution.

merge the data from all the sensor packages to improve the statistical accuracy, measurements of ϵ and C_T^2 were converted to the normalized variable

$$z = (\ln x - \langle \ln x \rangle)/\sigma_{\ln x}, \tag{11}$$

where x denotes either ϵ or C_T^2, and $\langle \ln x \rangle$ and $\sigma_{\ln x}$ denote the average and standard deviation of $\ln x$ over 3 min of data. The PDF of z using 0.25 s estimates of ϵ and C_T^2 from 10.0 to 11.5 UTC are shown in Figs. 3 and 4, respectively, as well as the predicted Gaussian distribution, that is, a lognormal distribution for ϵ and C_T^2. The agreement is excellent for ϵ and good for C_T^2, reflecting the larger variability in the temperature field. The lognormal PDF can also be produced from estimates with longer time averages, thus validating this ubiquitous result. However, the statistical accuracy of the histograms from longer time averages are reduced because of the smaller number of total estimates. The lognormal PDF of ϵ and C_T^2 agrees with previous surface layer measurements (Van Atta and Chen 1970; Kukharets 1988; Bezverkhniy et al. 1986, 1988; Frehlich 1992). We believe our results are the first reported for the shear region of a nocturnal jet.

4. Joint PDF of ϵ and C_T^2

It is natural to extend the assumption of a lognormal distribution for ϵ and C_T^2 to the assumption of a joint lognormal distribution (Van Atta 1971). The verification of a model for a joint PDF also requires a large number of measurements to sample the possible values of the joint random process. To increase the number of measurements we consider the normalized random variables

$$x = (\ln\epsilon - \langle \ln\epsilon \rangle)/\sigma_{\ln\epsilon}, \tag{12}$$

$$y = (\ln C_T^2 - \langle \ln C_T^2 \rangle)/\sigma_{\ln C_T^2}, \tag{13}$$

and write the joint normal PDF as

$$\mathrm{PDF}(x, y) = \frac{1}{2\pi(1-\rho^2)^{1/2}} \times \exp\left[-\frac{x^2 + y^2 - 2\rho xy}{2(1-\rho^2)}\right], \tag{14}$$

where ρ is the correlation coefficient between x and y. The conditional PDF of y given the values x is given by

$$\mathrm{PDF}(x|y) = \frac{1}{[2\pi(1-\rho^2)]^{1/2}} \exp\left[-\frac{(x-\rho y)^2}{2(1-\rho^2)}\right], \tag{15}$$

which is a normal distribution with mean ρy and variance $1 - \rho^2$. Examples of the conditional PDF $(x|y)$ are shown in Fig. 5, for all the measurements of ϵ and C_T^2 used in Figs. 3 and 4. The interval Δ around the conditional value y was chosen as $\Delta = 0.1$ for $y = 0.0$, -0.5, -1.0 and $\Delta = 0.2$ for $y = -1.5$. Similar results are produced for the PDF $(y|x)$. These results support the assumption of a joint lognormal distribution for ϵ and C_T^2.

5. Spatial spectrum of ϵ and C_T^2

The spatial spectra of ϵ and C_T^2 are estimated assuming Taylor's frozen turbulence hypothesis (Taylor 1938; Wyngaard and Clifford 1977; Hill 1996) to convert temporal frequency to spatial frequency. An estimate for

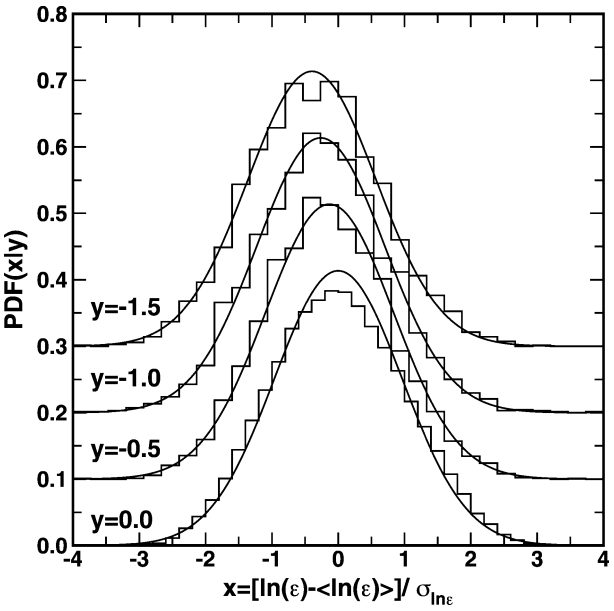

FIG. 5. Estimates of the conditional probability density function PDF $(x|y)$ and the prediction of the lognormal distribution, Eq. (15), for the measured value of $\rho = 0.264$ and various values of y. Each PDF is offset by 0.1.

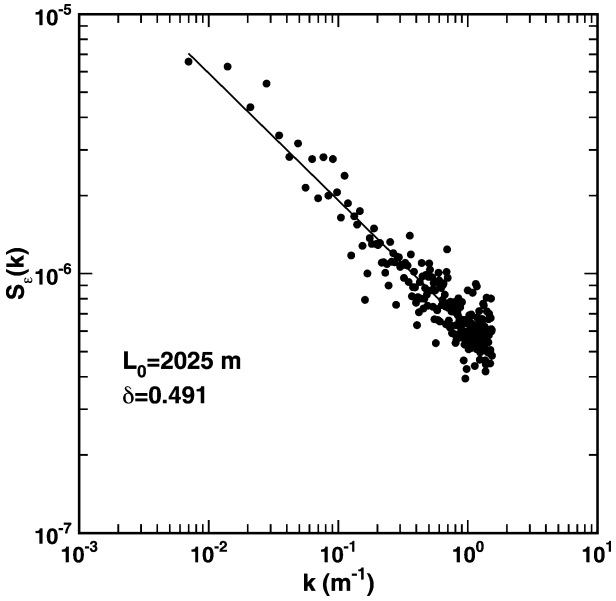

FIG. 6. Estimates of the spectrum $S_\epsilon(k)$ (•) and the maximum likelihood fit to the model Eq. (24) (solid line) for sensor package 5.

the temporal spectrum $S_x(f)$ of the random process $x(t)$ is given by the average of the periodogram

$$\hat{S}_x(n\Delta_f) = \frac{2\Delta_t}{M}\left|\sum_{m=0}^{M-1} x(m\Delta_t)e^{-2\pi inm/M}\right|^2, \qquad (16)$$

where f is the temporal frequency, Δ_t is the sampling interval for $x(t)$, M is the number of data points for each periodogram, Δ_f is the sampling interval in the frequency domain; that is,

$$\Delta_t\Delta_f = 1/M. \qquad (17)$$

Estimates $\hat{\epsilon}(m\Delta_t)$ and $\hat{C}_T^2(m\Delta_t)$ are produced (Frehlich et al. 2003) by fitting the spectral estimates of the longitudinal velocity $u(t)$ and temperature $T(t)$ over the time interval Δ_t, which can be as short as 0.25. These estimates can then be written as

$$\hat{x}(m\Delta_t) = \overline{x}(m\Delta_t) + \xi(m), \qquad (18)$$

where x denotes either ϵ or C_T^2:

$$\overline{x}(t) = \frac{1}{\Delta_t}\int_{t-\Delta_t/2}^{t+\Delta_t/2} x(t')\,dt' \qquad (19)$$

is the average of $x(t)$ over the sampling interval Δ_t and $\xi(m)$ is the estimation error of the measurement $\hat{x}(m\Delta_t)$. If the estimation error is uncorrelated with $x(t)$ then the ensemble average of the spectral estimates is given by

$$\langle\hat{S}_x(f)\rangle = S_x(f)H_A^2(f) + S_\xi(f), \qquad (20)$$

where

$$H_A(f) = \frac{\sin(\pi f\Delta_t)}{\pi f\Delta_t} \qquad (21)$$

is the frequency response of the averaging filter Eq. (19) and $S_\xi(f)$ is the spectrum of the estimation error $\xi(m)$. Therefore, an unbiased estimate of the spectrum $S_x(f)$ is given by

$$\hat{S}_{x\text{cor}}(n\Delta_f) = \frac{\hat{S}_x(n\Delta_f)}{H_A^2(n\Delta_f)}, \qquad (22)$$

which is a good approximation when the contribution from the noise spectrum $S_\xi(f)$ is negligible. Estimates for the spatial spectrum are given by the average of

$$\hat{S}_x(k) = \frac{U}{2\pi}\hat{S}_{x\text{cor}}\left[\frac{kU}{(2\pi)}\right], \qquad (23)$$

where U is the average wind speed over the measurement time $M\Delta_t$. Estimates of the spatial spectra were produced by computing the periodograms $\hat{S}_x(k)$ over 3-min sections of data, interpolating the results to a fixed wavenumber array, and averaging the interpolated periodograms over the total length of data. The results from package 5 located at 58-m altitude are shown in Figs. 6 and 7 for ϵ and C_T^2, respectively. The spectra are fit with the maximum likelihood estimator (Ruddick et al. 2000) to the model

$$S_x(k) = C(L_0^{-2} + k^2)^{-\delta/2}, \qquad (24)$$

where $\delta = 1 - \mu$ is the slope of the spectra, μ is the intermittency exponent, and L_0 is a length scale for the fluctuations of x. The spatial spectrum of ϵ has $\delta \approx 0.5$, which agrees with previous results from surface layer measurements (Gibson et al. 1970; Van Atta and Chen 1970). Praskovsky and Oncley (1994) estimated $\delta \approx 0.8$ for atmospheric surface layer measurements. The spatial spectrum of C_T^2 has $\delta \approx 0.6$, a value twice as

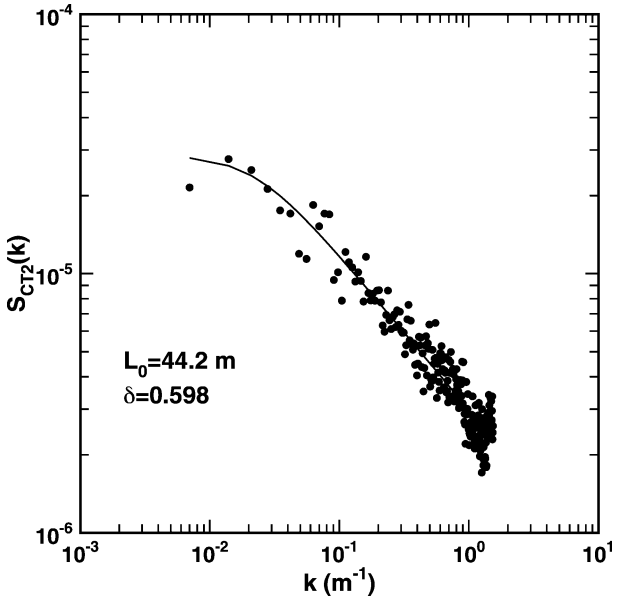

FIG. 7. Estimates of the spectrum $S_{CT2}(k)$ (•) and the maximum likelihood fit to the model Eq. (24) (solid line) for sensor package 5.

large as the $\delta \approx 0.3$ value determined by Kukharets (1988).

6. Summary and discussion

The variations in small-scale turbulence have a simple statistical description for the stationary conditions in the shear region below a low-level nocturnal jet observed during CASES-99. The small-scale turbulence is determined from maximum-likelihood estimates of the inertial range level of the spectra for short time intervals of data assuming no intermittency; that is, the spectra have a slope of $-5/3$ or equivalently the structure functions have a slope of 2/3 (Frehlich et al. 2003). The measurements in Fig. 1 do not indicate any statistically significant deviation from the 2/3 slope. Including the effects of intermittency, the second-order structure function would have a slope of $2/3 + \mu/9$ where μ is the intermittency exponent (Yaglom 1966). If $\mu = 0.5$, then a measurement accuracy for the slope must be better than 0.3846% to produce a 5% error bar for the exponent μ. This is a very difficult measurement because of the correlated nature of the errors in a structure function measurement. The results in Fig. 1 are consistent with $\mu = 0$ and with other measurements in high Reynolds number flow, for example, Praskovsky and Oncley (1994). This appears to be an unresolved issue for high Reynolds number flow. Since the intermittency correction is small, and if it is indeed required, the effects on the statistical variability of the small-scale turbulence would be negligible.

The probability density function of the energy dissipation rate ϵ and the temperature structure constant C_T^2 for small observation intervals (0.25–2.0 s or 1–8 m) are well approximated as lognormal distributions. This is consistent with previous measurements in the surface layer as well as aircraft measurements at higher altitudes (Nastrom and Gage 1985). The joint probability density function of ϵ and C_T^2 is also well approximated as a joint lognormal distribution. Accurate estimates of the joint PDF requires a large amount of data for statistically similar conditions. We increased the available dataset by using normalized random variables for conditions with approximately constant correlation coefficient ρ. More work is required to validate the joint lognormal approximation for various parameter regimes.

The spatial spectrum of ϵ and C_T^2 have a power-law dependence $k^{-\delta}$ in the inertial range. The power-law slope $\delta \approx 0.5$ for the spectrum of ϵ agrees with past surface layer measurements (Van Atta and Chen 1970; Gibson et al. 1970). However, for atmospheric surface layers, Pond and Stewart (1965) produced an estimate $\delta \approx 0.62$. Predictions of the spectral slope $\delta = 1 - \mu$ from estimates of the intermittency exponent μ based on other statistical quantities can produce different values; for example, Praskovsky and Oncley (1994) produced $\delta \approx 0.8$. These different power-law predictions have been explained by Nelkin (1981) and reconciled by Sreenivasan and Kailasnath (1993). Accurate small-scale turbulence measurements in a variety of locally stationary high Reynolds number flows are required to determine the nature of the intermittency. A lognormal random process is completely described by the spatial spectrum, or equivalently, the spatial correlation (Frehlich 1992). We believe our results are the first reported for the shear region of a low-level jet.

Acknowledgments. The authors acknowledge the useful suggestions of Andreas Muschinski. This work was supported by NSF and Army Research Office.

REFERENCES

Alisse, J., and C. Sidi, 2000: Experimental probability density functions of small-scale fluctuations in the stably stratified atmosphere. *J. Fluid Mech.,* **402,** 137–162.

Balsley, B. B., M. L. Jensen, and R. G. Frehlich, 1998: The use of state-of-the-art kites for profiling the lower atmosphere. *Bound.-Layer Meteor.,* **87,** 1–25.

——, ——, ——, Y. Meillier, and A. Muschinski, 2003: Structure and evolution of mean and turbulence characteristics of the nighttime lower troposphere above Kansas in the presence of a low-level jet. *J. Atmos. Sci.,* **60,** 2496–2508.

Bezverkhniy, V. A., A. S. Gurvich, and V. P. Kukharets, 1986: Variability of temperature fluctuation spectra in the atmospheric boundary layer. *Izv. Acad. Sci. USSR, Atmos. Oceanic Phys.,* **22,** 523–528.

——, ——, T. I. Makarova, and M. Z. Kholmyanskiy, 1988: Variation of local temperature and wind surface speed spectra in the atmospheric surface layer. *Izv. Acad. Sci. USSR, Atmos. Oceanic Phys.,* **24,** 519–527.

Cohn, S. A., 1995: Radar measurements of turbulent eddy dissipation rate in the troposphere: A comparison of techniques. *J. Atmos. Oceanic Technol.,* **12,** 85–95.

Eaton, F. D., S. A. McLaughlin, and J. R. Hines, 1995: A new fre-

quency-modulated continuous wave radar for studying planetary boundary layer morphology. *Radio Sci.,* **30,** 75–88.
Frehlich, R., 1992: Laser scintillation measurements of the temperature spectrum in the atmospheric surface layer. *J. Atmos. Sci.*, **49,** 1494–1509.
——, S. M. Hannon, and S. W. Henderson, 1998: Coherent Doppler lidar measurements of wind field statistics. *Bound.-Layer Meteor.*, **86,** 233–256.
——, Y. Meillier, M. L. Jensen, and B. Balsley, 2003: Turbulence measurements with the CIRES tethered lifting system during CASES-99: Calibration and spectral analysis of temperature and velocity. *J. Atmos. Sci.,* **60,** 2487–2495.
Frisch, U., 1995: *Turbulence: The Legacy of A. N. Kolmogorov*. Cambridge University Press, 296 pp.
Gibson, C. H., G. R. Stegen, and S. McConnell, 1970: Measurements of the universal constant in Kolmogoroff's third hypothesis for high Reynolds number turbulence. *Phys. Fluids*, **10,** 2448–2451.
Gossard, E. E., W. D. Neff, R. J. Zamora, and J. E. Gaynor, 1984: The find structure of elevated refractive layers: Implications for over-the-horizon propagation and radar sounding systems. *Radio Sci.,* **19,** 1523–1533.
Hill, R. J., 1996: Corrections to Taylor's frozen turbulence approximation. *Atmos. Res.,* **40,** 153–175.
Jacoby-Koaly, S., B. Campistron, S. Bernard, B. Bénech, F. Ardhuin-Girard, J. Dessens, E. Dupont, and B. Carissimo, 2002: Turbulent dissipation rate in the boundary layer via UHF wind profiler Doppler spectral width measurements. *Bound.-Layer Meteor.*, **103,** 361–389.
Kolmogorov, A. N., 1941: The local structure of turbulence in incompressible viscous fluid for very large Reynolds numbers. *Dokl. Akad. Nauk SSSR,* **30,** 299–303.
——, 1962: A refinement of previous hypotheses concerning the local structure turbulence in a viscous incompressible fluid at high Reynolds number. *J. Fluid. Mech.*, **13,** 82–85.
Kukharets, V. P., 1988: Investigation of variability of the structure characteristic of temperature in the atmospheric boundary layer. *Izv. Acad. Sci. USSR, Atmos. Oceanic Phys.,* **24,** 578–582.
Mahrt, L., 1989: Intermittency of atmospheric turbulence. *J. Atmos. Sci.,* **46,** 79–95.
Mandelbrot, B. B., 1991: Random multifractals: Negative dimensions and the resulting limitations of the thermodynamic formalism. *Proc. Roy. Soc. London,* **434A,** 79–88.
Monin, A. S., and A. M. Yaglom, 1975: *Statistical Fluid Mechanics: Mechanics of Turbulence.* Vol. 2. MIT Press, 874 pp.
Muschinski, A., and D. H. Lenschow, 2001: Future directions for research on meter- and submeter-scale atmospheric turbulence. *Bull. Amer. Meteor. Soc.,* **82,** 2831–2843.
——, R. Frehlich, M. L. Jensen, R. Hugo, A. Hoff, F. Eaton, and B. Balsley, 2001: Fine-scale measurements of turbulence in the lower troposphere: An intercomparison between a kite- and balloon-borne, and a helicopter-borne measurement system. *Bound.-Layer Meteor.,* **98,** 219–250.
Nastrom, G. D., and K. S. Gage, 1985: A climatology of atmospheric wavenumber spectra of wind and temperature observed by commercial aircraft. *J. Atmos. Sci.,* **42,** 950–960.
Nelkin, M., 1981: Do the dissipation fluctuations in high Reynolds number turbulence define a universal exponent? *Phys. Fluids*, **24,** 556–557.
Novikov, E. A., and R. W. Stewart, 1964: Intermittency of turbulence and the spectrum of fluctuations in energy dissipation. *Izv. Akad. Nauk. SSSR, Ser. Geofiz.*, **3,** 408–413.
Pond, S., and R. W. Stewart, 1965: Measurements of the statistical characteristics of small-scale turbulent motions (in Russian). *Izv. Atmos. Oceanic Phys.*, **1,** 914–919.
Poulos, G. S., and Coauthors, 2002: CASES-99: A comprehensive investigation of the stable nocturnal boundary layer. *Bull. Amer. Meteor. Soc.*, **83,** 555–581.
Praskovsky, A., and S. Oncley, 1994: Measurements of the Kolmogorov constant and intermittency exponent at very high Reynolds numbers. *Phys. Fluids*, **6,** 2886–2888.
Richter, J. H., 1969: High resolution tropospheric radar sounding. *Radio Sci.,* **4,** 1261–1268.
Roddier, F., 1981: The effects of atmospheric turbulence in optical astronomy. *Prog. Opt.,* **19,** 280–376.
Ruddick, B., A. Anis, and K. Thompson, 2000: Maximum likelihood spectral fitting: The Batchelor spectrum. *J. Atmos. Oceanic Technol.,* **17,** 1541–1555.
Smalikho, I. N., 1997: Accuracy of the turbulent energy dissipation rate estimation from the temporal spectrum of wind fluctuations. *Atmos. Oceanic Opt.,* **10,** 559–563.
Smedman, A.-S., 1988: Observation of a multi-level turbulence structure in a very stable atmospheric boundary layer. *Bound.-Layer Meteor.*, **44,** 231–253.
Sreenivasan, K. R., and P. Kailasnath, 1993: An update on the intermittency exponent in turbulence. *Phys. Fluids*, **5,** 512–514.
——, and G. Stolovitzky, 1996: Statistical dependence of inertial range properties on large scales in a high-Reynolds-number shear flow. *Phys. Rev. Lett.,* **77,** 2218–2221.
Tatarskii, V. I., 1971: *The Effects of the Turbulent Atmosphere on Wave Propagation.* Keter, 472 pp.
Taylor, G. I., 1938: The spectrum of turbulence. *Proc. Roy. Soc. London,* **A132,** 476–490.
Tyson, R. K., 1991: *Principles of Adaptive Optics.* Academic Press, 298 pp.
Van Atta, C. W., 1971: Influence of fluctuations in local dissipation rates on turbulent scalar characteristics in the inertial subrange. *Phys. Fluids*, **14,** 1803–1804.
——, and W. Y. Chen, 1970: Structure functions of turbulence in the atmospheric boundary layer over the ocean. *J. Fluid Mech.,* **44,** 145–159.
Wyngaard, J. C., and S. F. Clifford, 1977: Taylor's hypothesis and high-frequency turbulence spectra. *J. Atmos. Sci.,* **34,** 922–929.
Yaglom, A. M., 1966: The influence of fluctuations in energy dissipation on the shape of turbulence characteristics in the inertial interval. *Sov. Phys. Dokl.,* **11,** 26–29.